Acta Med. Okayama, 2024
Vol. 78, No. 1, pp. 29–36

Acta Medica Okayama
http://escholarship.lib.okayama-u.ac.jp/amo/

Original Article

Regression of Necrotic Lesions after Methotrexate Withdrawal in Patients with Methotrexate-Associated Lymphoproliferative Disorders: A Retrospective CT Study

Takahiro Kitayama[a]*, Takashi Tanaka[b], Yuichiro Kanie[c], Yohei Marukawa[d], Katsuhide Kojima[c], Takehiro Tanaka[e], Soshi Takao[f] and Takao Hiraki[a,g]

Departments of [a]Radiology, [e]Pathology, Graduate School of Medicine, Dentistry and Pharmaceutical Sciences, Okayama University, [c]Department of Radiology, Okayama University Hospital, Departments of [f]Epidemiology, [g]Radiology, Faculty of Medicine, Dentistry and Pharmaceutical Sciences, Okayama University, Okayama 700-8558, Japan, [b]Department of Radiology, Okayama City Hospital, Okayama 700-8557, Japan, [d]Department of Radiology, Okayama Saiseikai General Hospital, Okayama 700-8511, Japan

This retrospective study investigated whether necrotic lesions detected on a computed tomography (CT) scan are more regressive than non-necrotic lesions after methotrexate withdrawal in patients pathologically diagnosed with methotrexate-associated lymphoproliferative disorders (MTX-LPD). In total, 89 lesions extracted from 24 patients on CT scans were included in the analysis. All patients had been evaluated for the presence of necrosis within lesions via CT scan upon first suspicion of MTX-LPD (baseline CT scan). The percentage lesion size reduction between the baseline and initial follow-up CT scan was calculated. The association between necrosis within lesions and size changes was estimated via linear regression analyses using both crude and adjusted models. Necrosis was significantly more common in extranodal lesions (27 out of 30 lesions, 90%) than in nodal lesions (9 out of 59 lesions, 15%, $p < 0.001$). In the crude model, the regression of necrotic lesions was 58.5% greater than that of non-necrotic lesions; the difference was statistically significant ($p < 0.001$). Additionally, the longest diameter of necrotic lesions at the baseline CT scan was significantly greater than that of non-necrotic lesions ($p < 0.001$). Based on the adjusted model, necrotic lesions showed 49.3% greater regression than non-necrotic lesions ($p = 0.017$). Necrosis detected on a CT scan was found to be an independent predictor of regression after MTX withdrawal in patients with MTX-LPD.

Key words: methotrexate, lymphoproliferative disorder, computed tomography, necrosis

Methotrexate-associated lymphoproliferative disorders (MTX-LPD) are rare benign lymphoid proliferations or malignant lymphomas that occur predominantly in patients with rheumatoid arthritis against a background of immunodeficiency caused by treatment with MTX. The prominent clinical characteristic of MTX-LPD is regression after MTX withdrawal. Therefore, MTX withdrawal is the initial step for managing clinically suspected MTX-LPD [1-5].

Thus far, several prognostic factors have been reported. A clinicopathological study of MTX-LPD showed that histological subtype and age are correlated with overall survival [4]. Similarly, histological subtype has also been reported to be associated with spontaneous regression after MTX withdrawal [6]. In addi-

Received April 28, 2023; accepted August 9, 2023.
*Corresponding author. Phone: +81-86-235-7313; Fax: +81-86-235-7316
E-mail: kitayama-t@s.okayama-u.ac.jp (T. Kitayama)

Conflict of Interest Disclosures: No potential conflict of interest relevant to this article was reported.

tion, tumor necrosis detected via pathological investigation is a favorable factor for progression-free survival in different subtypes of MTX-LPD [7]. Using diagnostic imaging, other studies found that necrosis detected on computed tomography (CT) scans correlates with poor prognosis in some subtypes of *de novo* lymphoma [8,9]. In contrast, there are no reports on the predictive value of lesion necrosis detected on a CT scan in MTX-LPD.

At present, there is no strict guideline for the management of MTX-LPD. Diagnostic imaging aims primarily to evaluate the presence and extent of MTX-LPD lesions and to monitor the prevalence of lesions after MTX withdrawal. Imaging findings may also be used as biomarkers for predicting the regression of MTX-LPD lesions after MTX withdrawal.

In this study, we hypothesized that lesion necrosis detected on a CT scan was correlated with regression after MTX withdrawal in patients with MTX-LPD. The present study aimed primarily to investigate whether necrotic lesions detected on CT scans are more regressive than non-necrotic lesions after MTX withdrawal in patients pathologically diagnosed with MTX-LPD. Moreover, the characteristics of the lesions associated with regression after MTX withdrawal were evaluated.

Materials and Methods

This retrospective and observational study was approved by our institutional review board; informed consent was waived due to the retrospective nature of the research (approval no. Ken2108-019).

Participants. Using radiology information systems, we identified all patients who met a single inclusion criterion: suspected MTX-LPD on a CT scan performed from January 2011 to December 2020. Sixty consecutive patients met the criterion. Out of the 60 patients, 36 patients were excluded for the following reasons: no CT scan before or after MTX withdrawal (n = 14); non-evaluable lesions due to poor image quality (n = 8); diagnosis of other pathologies (*i.e.*, infectious lesion or malignant tumor other than lymphoma) (n = 5); no detectable lesions on CT scan (n = 3); no MTX withdrawal (n = 3); and no pathological confirmation (n = 3). The remaining 24 patients pathologically diagnosed with MTX-LPD were analyzed (Fig. 1).

Image acquisition. CT scans were performed using, among others, the following helical scanners: Discovery CT750 HD (GE Healthcare, Milwaukee, WI, USA); Aquilion ONE ViSION Edition (Canon Medical Systems, Ohtawara, Japan); SOMATOM Definition Flash (Siemens Healthineers, Forchheim, Germany); Aquilion 64 (Canon Medical Systems); Aquilion MULTI (Canon Medical Systems). In total, 15 patients underwent a contrast-enhanced CT scan. The volume of iodinated contrast agent used with 300 mg of iodine per milliliter was 2-2.5 ml/kg. The contrast agent was administered via a mechanical injector within 50 sec with a scanning delay of 70 sec. The other 9 patients underwent an unenhanced CT scan. Based on our

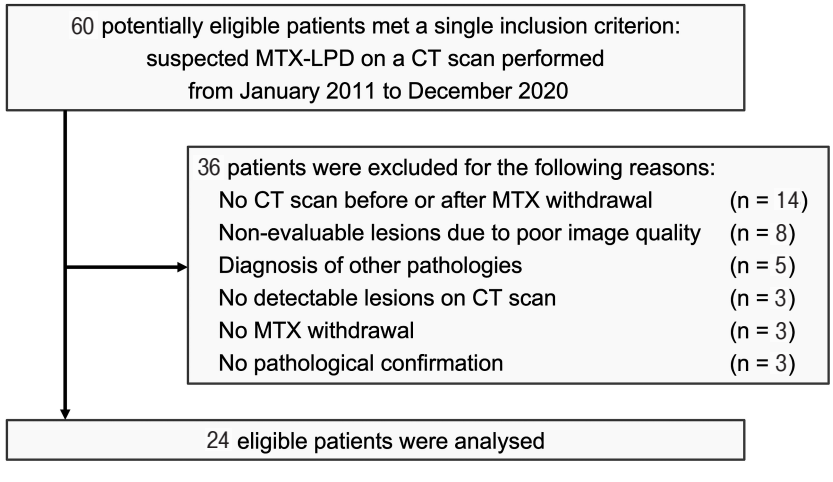

Fig. 1 Flow diagram for patient inclusion.
MTX-LPD, methotrexate-associated lymphoproliferative disorders; CT, computed tomography.

standard imaging protocol, the following parameters were used: 120 kilovolt peak, automated tube current modulation mode, a beam pitch of 1.0, gantry rotation time of 0.5 sec, and field of view to fit. The images were reconstructed using axial planes with a 5 mm section thickness. To evaluate necrosis within lesions, all images were displayed using the soft tissue window settings (level: 30 Hounsfield units [HU]; width: 350 HU). To measure lung lesions and other lesions, the lung window settings (level: −550HU; width: 1,500 HU) and the soft tissue window settings were used, respectively.

Image analysis and regression assessment. The target lesions were defined according to the Lugano Response Criteria [10]. The number of target lesions per patient was up to 6 of the largest nodal or extranodal lesions detected by the baseline CT scan performed upon MTX-LPD suspicion. Abnormal lymph nodes were classified as lesions with a long axis measuring > 1.5 cm, while extranodal lesions were defined as those with a long axis measuring > 1.0 cm. Non-mass lesions, such as splenomegaly, hepatomegaly, and bone marrow involvement, were not considered target lesions.

We evaluated necrosis within the lesions at the baseline CT scan upon MTX-LPD suspicion, following the protocol used in a previous study that evaluated tumor necrosis on CT scan in malignant lymphoma [8]. In patients who underwent unenhanced CT scan, necrosis was defined as a visual focal area of low attenuation within nodal or extranodal lesions with corresponding HU measuring between 10 and 30 HU. In addition, for patients who underwent a contrast-enhanced CT scan, a corresponding area without a significant HU increase (up to a maximum of 5 HU) between the unenhanced and contrast-enhanced scans was required. Size-adjustable oval region-of-interest analysis was performed, and the corresponding HU values measured at the center of the necrotic area were investigated. Necrosis was independently evaluated by two experienced diagnostic radiologists, neither of whom was the radiologist who assessed the target lesion size. These readers were blinded to any additional clinical and pathological information, including images obtained via other modalities. All lesions were evaluated as positive or negative. In this study, we defined true necrosis based on the necrotic findings on CT scan alone. If there was discordance between the two readers, a consensus was achieved via discussion.

Regression was assessed during the initial follow-up CT scan after MTX withdrawal and the baseline CT scan performed upon MTX-LPD suspicion. The percentage lesion size reduction was calculated according to differences in the product of the longest and perpendicular diameters between the baseline and the follow-up CT scans, divided by the product of the diameters at baseline CT scan, in line with previous studies that evaluated changes in tumor size on CT scans in malignant lymphoma [10-12].

Assessment of pathologic and clinical data. Histopathological diagnosis was determined based on the World Health Organization classification, revised 4th edition (2017) [13]. Pathological confirmation was achieved through hematoxylin and eosin staining, immunohistochemical staining, flow cytometry analysis, and *in situ* hybridization of Epstein–Barr virus encoding ribonucleic acid. An experienced pathologist confirmed all histopathological diagnoses. Patient stage was determined based on the Lugano classification system for malignant lymphoma [10]. Table 1 shows the characteristics of the patients in detail. There were no significant differences in patient characteristics between the groups of patients who had no necrotic lesions and those who had at least one.

Statistical analysis. Descriptive data were presented as means ± standard deviation (SD) and range for continuous variables, and as counts for categorical variables. Systemic target lesions were divided into nodal or extranodal anatomic regions, which was similar to the classification used in previous region-based analyses of lymphoproliferative disorders [14-17]. The percentages of lesion size reduction between necrotic and non-necrotic lesions were compared. Continuous variables with a normal distribution were estimated using the *t*-test. Differences between categorical variables were evaluated using Fisher's exact test (for expected group sizes of ≤ 5). Linear regression analyses were used to estimate beta coefficients with 95% confidence intervals of crude and adjusted models. In the adjusted model, we controlled for lesion site (nodal or extranodal) and size (the product of the longest and perpendicular diameters at baseline CT scan). For each analysis, a two-tailed $p < 0.05$ was considered statistically significant. All statistical analyses were performed using Stata Statistical Software Release 17.0 (Stata Corp LLC, College Station, TX, USA).

Table 1 Characteristics of patients with MTX-LPD (n = 24)

	All patients (n = 24)	Necrosis status		*P*-value
		Necrosis (−)[a] (n = 9)	Necrosis (+)[b] (n = 15)	
Age, years, mean ± SD (range)	69.5 ± 9.2 (39–90)	71.0 ± 5.2 (64–80)	68.5 ± 10.9 (39–90)	0.535
Gender, n				0.351
Male	6	1	5	
Female	18	8	10	
Underlying disease, n				0.375
RA	23	8	15	
Others[c]	1	1	0	
Length of MTX, months, mean ± SD (range)	115.8 ± 109.4 (26–396)	90.6 ± 125.2 (26–396)	131.2 ± 100.6 (47–360)	0.423
Final dose of MTX, mg/week, mean ± SD (range)	8.5 ± 3.1 (2.5–14)	6.8 ± 1.8 (4–10)	9.4 ± 3.3 (2.5–14)	0.0502
Combination with other immunosuppressive drugs[d], n	15	5	10	0.678
sIL-2R, U/ml, mean ± SD (range)	1,676.6 ± 1,259.3 (343–4,728)	1,730.3 ± 1,503.2 (343–4,728)	1,644.4 ± 1,145.0 (476–4,511)	0.876
LDH, U/l, mean ± SD (range)	303.0 ± 106.1 (183–576)	286.7 ± 128.4 (192–576)	312.9 ± 93.8 (183–518)	0.570
Histological type, n				0.100
Malignant	23	8	15	
DLBCL	16	4	12	
FL	2	1	1	
HL	2	1	1	
MZL	2	2	0	
PTCL	1	0	1	
Benign	1	1	0	
EBER, n				1.00
Positive	14	4	10	
Negative	7	2	5	
N/A	3	3	0	
Stage[e], n				0.182
I	3	2	1	
II	4	2	2	
III	5	3	2	
IV	12	2	10	
Use of contrast agent at baseline CT scan[f], n				0.678
Contrast-enhanced scan	15	5	10	
Unenhanced scan	9	4	5	
Interval between baseline CT scan[f] and MTX withdrawal, day, mean ± SD (range)	9.0 ± 8.5 (0–33)	6.0 ± 3.7 (1–12)	10.9 ± 10.1 (0–33)	0.182
Interval between MTX withdrawal and follow-up CT scan[g], day, mean ± SD (range)	38.2 ± 28.2 (3–101)	41.3 ± 23.7 (3–67)	36.3 ± 31.2 (3–101)	0.684

MTX-LPD, methotrexate-associated lymphoproliferative disorders; SD, standard deviation; RA, rheumatoid arthritis; sIL-2R, soluble interleukin-2 receptor; LDH, lactate dehydrogenase; DLBCL, diffuse large B-cell lymphoma; FL, follicular lymphoma; HL, Hodgkin lymphoma; MZL, marginal zone lymphoma; PTCL, peripheral T-cell lymphoma; EBER, *in situ* hybridisation of Epstein–Barr virus encoding ribonucleic acid; N/A, not available; CT, computed tomography.

[a]Patients who have no necrotic lesions, [b]Patients who have at least one necrotic lesion, [c]One patient with coexisting polymyositis and Sjögren's syndrome, [d]E.g., prednisolone, tacrolimus and salazosulfapyridine, [e]Lugano classification system, [f]CT scan upon MTX-LPD suspicion, [g]Initial follow-up CT scan after MTX withdrawal.

Results

Among 89 lesions, 36 with necrosis and 53 without were included in the analysis and were followed up. Table 2 presents the specific site of each nodal or extranodal lesion. Necrosis was identified within 9 (15%) of 59 nodal lesions and 27 (90%) of 30 extranodal lesions. Necrosis was significantly more common in extranodal lesions than in nodal lesions ($p < 0.001$).

Table 3 shows the percentage lesion size reduction based on the univariate analysis. The mean ± SD for the percentage size reduction in lesions without necrosis and those with necrosis were −10.5 ± 79.1% and 48.0 ± 24.1%, respectively. Necrotic lesions had more significant regression than non-necrotic lesions ($p < 0.001$). In addition, the mean ± SD of the longest diameter of non-necrotic lesions at baseline CT scan was 25.6 ± 7.3 mm, whereas it was 39.5 ± 20.9 mm for necrotic lesions, a significant difference ($p < 0.001$).

Table 4 shows the association between necrosis and the percentage lesion size reduction based on the linear regression analysis. In the model adjusted for lesion site (nodal or extranodal) and size (the product of the longest and perpendicular diameters at baseline CT scan), necrotic lesions regressed 49.3% (95% confidence interval: 9.0-89.6) more than non-necrotic lesions ($p = 0.017$); the difference was statistically significant. Figures 2 and 3 show respective representative images of necrotic and non-necrotic lesions.

Table 2 Specific site of each nodal or extranodal lesion (n = 89)

	Necrosis (−)[a] (n = 53)	Necrosis (+)[b] (n = 36)
Nodal, n	**50**	**9**
Neck[c]	7	2
Infraclavicular	1	0
Axillary and pectoral	11	1
Mediastinal	12	2
Hilar	1	1
Spleen	2	0
Paraaortic	6	3
Iliac	10	0
Extra nodal, n	**3**	**27**
Renal and adrenal	1	11
Lung	1	9
Skin/subcutaneous	0	6
Liver	0	1
Others[d]	1	0

CT, computed tomography; MTX-LPD, methotrexate-associated lymphoproliferative disorders.
[a]Lesions without necrosis on CT scan upon MTX-LPD suspicion, [b]Lesions with necrosis on CT scan upon MTX-LPD suspicion, [c]Included cervical, supraclavicular, occipital, and preauricular regions, [d]Thyroid.

Discussion

This retrospective study revealed that necrotic lesions detected on CT scans were more regressive than non-necrotic lesions after MTX withdrawal in patients with MTX-LPD. Lesion site and size at baseline CT scan were correlated with the presence of necrosis. However, multivariate analysis revealed that necrosis was a predictor of regression independent of these factors. Previous reports have found that MTX withdrawal is the initial step for managing MTX-LPD because some lesions regress after MTX withdrawal [1-5]. Immediate chemotherapy is not required in these patients, and the importance of predicting regression is underscored by the fact that the patients with MTX-LPD are usually older and immunocompromised and thus more at risk of adverse effects. This research emphasized the role of CT scan imaging in predicting

Table 3 Percentage lesion size reduction based on the univariate analysis

	Necrosis (−)[a] (n = 53)	Necrosis (+)[b] (n = 36)	*P*-value
Longest diameter at the baseline CT[c], mm, mean ± SD (range)	25.6 ± 7.3 (16–47)	39.5 ± 20.9 (16–107)	< 0.001[d]
Longest diameter at the follow-up CT[e], mm, mean ± SD (range)	25.1 ± 12.1 (0–51)	28.4 ± 18.7 (0–82)	0.318
Percentage lesion size reduction[f], %, mean ± SD (range)	−10.5 ± 79.1 (−284–100)	48.0 ± 24.1 (−4–100)	< 0.001[d]

CT, computed tomography; SD, standard deviation; MTX-LPD, methotrexate-associated lymphoproliferative disorders.
[a]Lesions without necrosis on CT scan upon MTX-LPD suspicion, [b]Lesions with necrosis on CT scan upon MTX-LPD suspicion, [c]CT scan upon MTX-LPD suspicion, [d]Statistically significant ($p < 0.05$), [e]Initial follow-up CT scan after MTX withdrawal, [f]Calculated according to differences in the product of the longest and perpendicular diameters between the baseline and the follow-up CT scans, divided by the product of the diameters at baseline CT scan.

Table 4 Association between necrosis and the percentage lesion size reduction[a] based on the linear regression analysis

	Crude model (n = 89)		Adjusted model[b] (n = 89)	
	Beta coefficients (95% CI), %	*P*-value	Beta coefficients (95% CI), %	*P*-value
Necrosis (−)[c]	–	–	–	–
Necrosis (+)[d]	58.5 (31.5–85.6)	< 0.001[e]	49.3 (9.0–89.6)	0.017[e]

CI, confidence interval; CT, computed tomography; MTX-LPD, methotrexate-associated lymphoproliferative disorders.

[a]Calculated according to differences in the product of the longest and perpendicular diameters between the baseline and the follow- up CT scans, divided by the product of the diameters at baseline CT scan, [b]Adjusted for lesion site (nodal or extranodal) and size (the product of the longest and perpendicular diameters at baseline CT scan), [c]Lesions without necrosis on CT scan upon MTX-LPD suspicion, [d]Lesions with necrosis on CT scan upon MTX-LPD suspicion, [e]Statistically significant ($p < 0.05$).

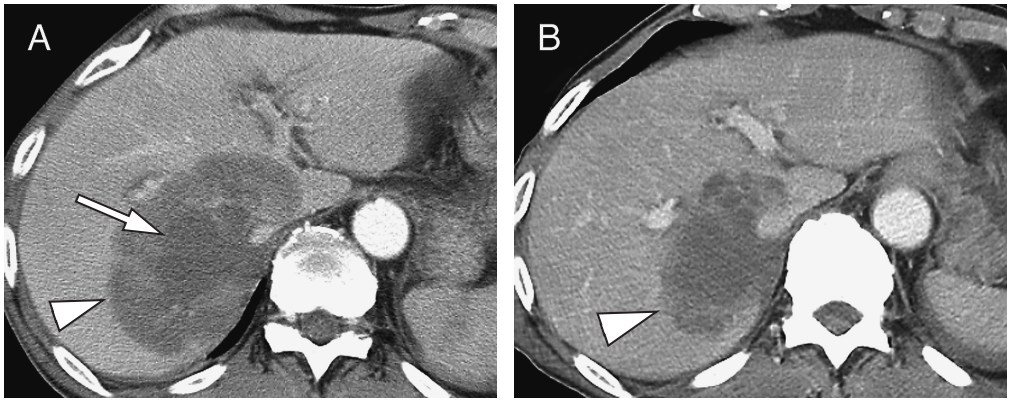

Fig. 2 Representative images of a necrotic lesion. **A**, A 74-year-old man presented with diffuse large B-cell lymphoma and extensive necrosis (arrow) at the center of the liver lesion (arrowhead) on a contrast-enhanced axial computed tomography scan before methotrexate withdrawal; **B**, Lesion size reduction (arrowhead) on follow-up contrast-enhanced axial computed tomography scan performed 3 days after methotrexate withdrawal.

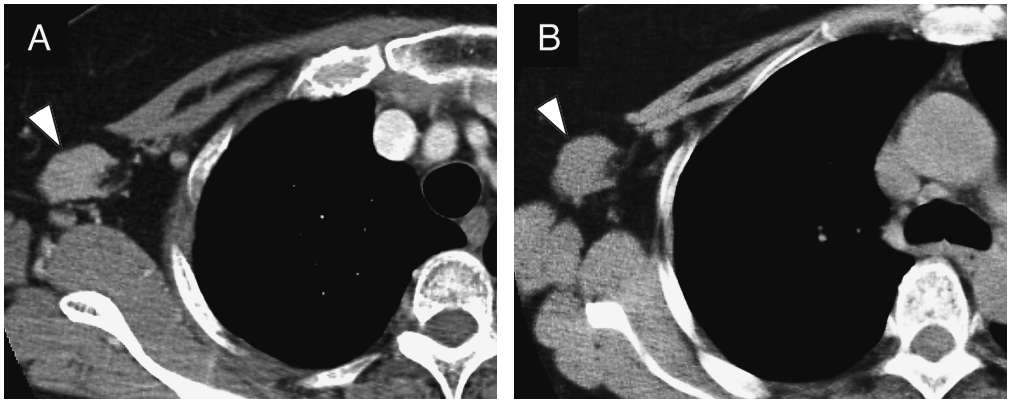

Fig. 3 Representative images of a non-necrotic lesion. **A**, 65-year-old woman presented with follicular lymphoma but without a necrotic area within the right axillary lesion (arrowhead) on a contrast-enhanced axial computed tomography scan before methotrexate withdrawal; **B**, No significant change in lesion size (arrowhead) on follow-up unenhanced axial computed tomography scan 56 days after methotrexate withdrawal.

regression after MTX withdrawal among patients with MTX-LPD.

Few studies have reported on diagnostic imaging predictors after MTX withdrawal in MTX-LPD. Takanashi *et al.* used the maximum standardized uptake value on ^{18}F-fluorodeoxyglucose positron emission tomography/computed tomography (FDG PET/CT) and the maximum size of MTX-LPD-associated tumors as predictors of spontaneous regression after MTX withdrawal [18]. Kameda *et al.* reported that the sum of the metabolic tumor volume and the sum of total lesion glycolysis on ^{18}F-FDG PET/CT can be used as predictors of spontaneous regression [19]. However, Watanabe *et al.* showed that none of the ^{18}F-FDG PET factors before MTX withdrawal could be used to predict clinical outcomes after MTX withdrawal [17]. Thus, predictors of regression after MTX withdrawal on diagnostic imaging remain controversial.

Previous studies have not reported on necrosis within lesions detected on CT scans in MTX-LPD. Only the study conducted by Kurita *et al.* assessed pathologically identified necrosis within lesions in MTX-LPD. Their results showed that necrosis was a significant factor for better progression-free survival in diffuse large B-cell lymphoma and a subspecific subtype of LPD lesions [7]. On the other hand, in *de novo* diffuse large B-cell lymphoma, patients with necrosis within lesions detected on CT scans had significantly worse progression-free survival and overall survival than those without necrosis [8]. Similarly, in *de novo* peripheral T-cell lymphoma, patients with necrosis within lesions detected on CT scans had significantly poorer outcomes (progression during therapy or lesion relapse within 24 months after therapy) than those without necrosis [9]. Thus, necrosis detected on CT scans is correlated with a poor prognosis in some subtypes of *de novo* lymphoma. Our results may help clinicians prevent unnecessary chemotherapy in patients with MTX-LPD who have necrotic lesions. Currently, it is unclear why necrotic lesions detected on CT scans are more regressive than non-necrotic lesions after MTX withdrawal in patients with MTX-LPD. We speculate that necrosis might reflect potential host immunity against MTX-LPD, but further studies to elucidate its etiology are desired.

Watanabe *et al.* observed extranodal involvement on ^{18}F-FDG PET/CT in 17 (18%) of 92 anatomic regions [17]. In our study, 30 (34%) of 89 lesions were identified in the extranodal regions. In several patient-based evaluations, extranodal involvement was observed in 40-50% of patients [1,2,7,19]. Furthermore, in our study, necrosis was identified on 36 (40%) of 89 lesions and was significantly more common within extranodal than within nodal lesions. In a clinicopathological study, Kurita *et al.* showed that 103 (48%) of 214 patients had extranodal involvement. Moreover, 56 (29%) of 192 lesions presented with pathologically identified necrosis, but the correlation between lesion site (nodal or extranodal) and frequency of necrosis was not reported [7]. The cause of this association is unclear. However, in our study, necrosis within lesions detected on CT scans was an independent predictor of regression based on the multivariate analysis.

To the best of our knowledge, only the study by Takanashi *et al.* evaluated the specific size of MTX-LPD lesions on ^{18}F-FDG PET/CT [18]. Their results showed that the mean maximum diameter of the largest tumors upon diagnosis was 30 mm (range: 10-110 mm) (n = 18). This was similar to our results, in which the mean longest diameter of all lesions at baseline CT scan was 31 mm (range: 16-107 mm). However, Takanashi *et al.* assessed the size of the largest lesion of each patient alone, and thus their results cannot be directly compared with ours. In addition, they reported that the maximum diameters of the spontaneous regression group were smaller than those of the nonspontaneous regression group (n = 5, mean = 20 mm; and n = 13, mean = 52 mm, respectively; $p = 0.04$). In contrast, our results showed that necrotic lesions were larger than non-necrotic lesions at baseline CT scan. However, our multivariate analysis showed that necrotic lesions had significantly more regression than non-necrotic lesions. The association between lesion size and regression thus remains unclear, and further prospective studies are warranted.

The present study had several limitations. First, we included various imaging modalities and protocols because of our study's retrospective nature. Second, the study cohort comprised a relatively small number of patients because of the rarity of this disease. Third, we did not consider non-mass lesions, such as splenomegaly, hepatomegaly, and bone marrow involvement, as target lesions. In clinical practice, a comprehensive assessment of these findings is required when evaluating regression after MTX withdrawal.

In conclusion, necrosis detected on a CT scan is an

independent predictor of spontaneous regression after MTX withdrawal in patients with MTX-LPD. The results of this study enhance the role of CT imaging in MTX-LPD in predicting regression after MTX withdrawal as well as in evaluating the extent of the lesions.

References

1. Salloum E, Cooper DL, Howe G, Lacy J, Tallini G, Crouch J, Schultz M and Murren J: Spontaneous regression of lymphoproliferative disorders in patients treated with methotrexate for rheumatoid arthritis and other rheumatic diseases. J Clin Oncol (1996) 14: 1943–1949.
2. Ichikawa A, Arakawa F, Kiyasu J, Sato K, Miyoshi H, Niino D, Kimura Y, Takeuchi M, Yoshida M, Ishibashi Y, Nakashima S, Sugita Y, Miura O and Ohshima K: Methotrexate/iatrogenic lymphoproliferative disorders in rheumatoid arthritis: histology, Epstein-Barr virus, and clonality are important predictors of disease progression and regression. Eur J Haematol (2013) 91: 20–28.
3. Inui Y, Matsuoka H, Yakushijin K, Okamura A, Shimada T, Yano S, Takeuchi M, Ito M, Murayama T, Yamamoto K, Itoh T, Aiba K and Minami H: Methotrexate-associated lymphoproliferative disorders: management by watchful waiting and observation of early lymphocyte recovery after methotrexate withdrawal. Leuk Lymphoma (2015) 56: 3045–3051.
4. Tokuhira M, Saito S, Okuyama A, Suzuki K, Higashi M, Momose S, Shimizu T, Mori T, Anan-Nemoto T, Amano K, Okamoto S, Takeuchi T, Tamaru JI and Kizaki M: Clinicopathologic investigation of methotrexate-induced lymphoproliferative disorders, with a focus on regression. Leuk Lymphoma (2018) 59: 1143–1152.
5. Tokuhira M, Tamaru JI and Kizaki M: Clinical management for other iatrogenic immunodeficiency-associated lymphoproliferative disorders. J Clin Exp Hematop (2019) 59: 72–92.
6. Gion Y, Iwaki N, Takata K, Takeuchi M, Nishida K, Orita Y, Tachibana T, Yoshino T and Sato Y: Clinicopathological analysis of methotrexate-associated lymphoproliferative disorders: Comparison of diffuse large B-cell lymphoma and classical Hodgkin lymphoma types. Cancer Sci (2017) 108: 1271–1280.
7. Kurita D, Miyoshi H, Ichikawa A, Kato K, Imaizumi Y, Seki R, Sato K, Sasaki Y, Kawamoto K, Shimono J, Yamada K, Muto R, Kizaki M, Nagafuji K, Tamaru JI, Tokuhira M and Ohshima K: Methotrexate-associated Lymphoproliferative Disorders in Patients With Rheumatoid Arthritis: Clinicopathologic Features and Prognostic Factors. Am J Surg Pathol (2019) 43: 869–884.
8. Adams HJA, de Klerk JMH, Fijnheer R, Dubois SV, Nievelstein RAJ and Kwee TC: Prognostic value of tumor necrosis at CT in diffuse large B-cell lymphoma. Eur J Radiol (2015) 84: 372–377.
9. Yang W, Jiang S, Lin J and Li Y: CT findings predict survival of patients with peripheral T cell lymphoma: a preliminary study. Radiol Oncol (2019) 53: 31–38.
10. Cheson BD, Fisher RI, Barrington SF, Cavalli F, Schwartz LH, Zucca E and Lister TA: Recommendations for initial evaluation, staging, and response assessment of Hodgkin and non-Hodgkin lymphoma: the Lugano classification. J Clin Oncol (2014) 32: 3059–3068.
11. Spira D, Vogel W, Sökler M, Löffler S, Sauter A, Schulze M and Horger M: Size and attenuation CT (SACT) of residual masses in patients with follicular non-Hodgkin lymphoma: more than a status quo? Eur J Radiol (2012) 81: 1657–1661.
12. Wei YC, Ding CY, Liang JH, Wang L, Zhu HY, Xia Y, Wu JZ, Fan L, Li TN, Li JY and Xu W: Interim response in diffuse large B cell lymphoma on CT: what is the optimal size reduction (Δ SPD) for predicting outcome? Eur Radiol (2020) 30: 3094–3100.
13. Swerdlow S, Campo E, Harris N, Jaffe E, Pileri S, Stein H, Thiele J, Arber D, Hasserjian R, Beau M, Orazi A and Siebert R: WHO classification of tumors of haematopoietic and lymphoid tissues, Revised 4th Ed, IARC, Lyon (2017).
14. Moon SH, Cho SK, Kim WS, Kim SJ, Chan Ahn Y, Choe YS, Lee KH, Kim BT and Choi JY: The role of 18F-FDG PET/CT for initial staging of nasal type natural killer/T-cell lymphoma: a comparison with conventional staging methods. J Nucl Med (2013) 54: 1039–1044.
15. London K, Cross S, Onikul E, Dalla-Pozza L and Howman-Giles R: 18F-FDG PET/CT in paediatric lymphoma: comparison with conventional imaging. Eur J Nucl Med Mol Imaging (2011) 38: 274–284.
16. Fueger BJ, Yeom K, Czernin J, Sayre JW, Phelps ME and Allen-Auerbach MS: Comparison of CT, PET, and PET/CT for staging of patients with indolent non-Hodgkin's lymphoma. Mol Imaging Biol (2009) 11: 269–274.
17. Watanabe S, Manabe O, Hirata K, Oyama-Manabe N, Hattori N, Kikuchi Y, Kobayashi K, Toyonaga T and Tamaki N: The usefulness of (18)F-FDG PET/CT for assessing methotrexate-associated lymphoproliferative disorder (MTX-LPD). BMC Cancer (2016) 16: 635.
18. Takanashi S, Nakazato T, Aisa Y, Ito C, Arakaki H, Osada Y, Hirano M and Mori T: The prognostic value of positron emission tomography/computed tomography in rheumatoid arthritis patients with methotrexate-associated lymphoproliferative disorders. Ann Hematol (2018) 97: 1611–1618.
19. Kameda T, Nakashima S, Mitamura K, Yamamoto Y, Norikane T, Shimada H, Wakiya R, Kato M, Miyagi T, Sugihara K, Mino R, Mizusaki M, Kadowaki N and Dobashi H: FDG-PET/CT imaging parameters for predicting spontaneous regression of methotrexate-associated lymphoproliferative disorder in patients with rheumatoid arthritis. Sci Rep (2022) 12: 15367.